

Diversity of the Supernova - Gamma-Ray Burst Connection

K. NOMOTO⁽¹⁾, N. TOMINAGA⁽¹⁾, M. TANAKA⁽¹⁾, K. MAEDA⁽²⁾, T. SUZUKI⁽¹⁾,
J.S. DENG⁽³⁾(¹), and P.A. MAZZALI⁽⁴⁾(⁵)(¹)

⁽¹⁾ *Department of Astronomy, University of Tokyo, Bunkyo-ku, Tokyo 113-0033, Japan*

⁽²⁾ *Department of Earth Science and Astronomy, College of Arts and Science, University of Tokyo, Meguro-ku, Tokyo 153-8902, Japan*

⁽³⁾ *National Astronomical Observatories, CAS, Beijing 100012, China*

⁽⁴⁾ *Max-Planck-Institut für Astrophysik, 85741 Garching, Germany*

⁽⁵⁾ *Istituto Nazionale di Astrofisica-OATs, Via Tiepolo 11, I-34131 Trieste, Italy*

Summary. —

The connection between the long Gamma Ray Bursts (GRBs) and Type Ic Supernovae (SNe) has revealed interesting diversity. We review the following types of the GRB-SN connection. (1) GRB-SNe: The three SNe all explode with energies much larger than those of typical SNe, thus being called Hypernovae (HNe). They are massive enough for forming black holes. (2) Non-GRB HNe/SNe: Some HNe are not associated with GRBs. (3) XRF-SN: SN 2006aj associated with X-Ray Flash 060218 is dimmer than GRB-SNe and has very weak oxygen lines. Its progenitor mass is estimated to be small enough to form a neutron star rather than a black hole. (4) Non-SN GRB: Two nearby long GRBs were not associated SNe. Such “dark HNe” have been predicted in this talk (i.e., just before the discoveries) in order to explain the origin of C-rich (hyper) metal-poor stars. This would be an important confirmation of the Hypernova-First Star connection. We will show our attempt to explain the diversity in a unified manner with the jet-induced explosion model.

PACS 98.70.Rz – gamma-ray bursts.

PACS 97.60.Bw – supernovae.

PACS 26.30.+k – Nucleosynthesis in supernovae.

To be published in the proceedings of the conference “SWIFT and GRBs: Unveiling the Relativistic Universe”, Venice, June 5-9, 2006. To appear in “Il Nuovo Cimento”

1. – Introduction

Long-duration γ -ray bursts (GRBs) at sufficiently close distances ($z < 0.2$) have been found to be accompanied by luminous core-collapse Type Ic supernovae (SNe Ic)

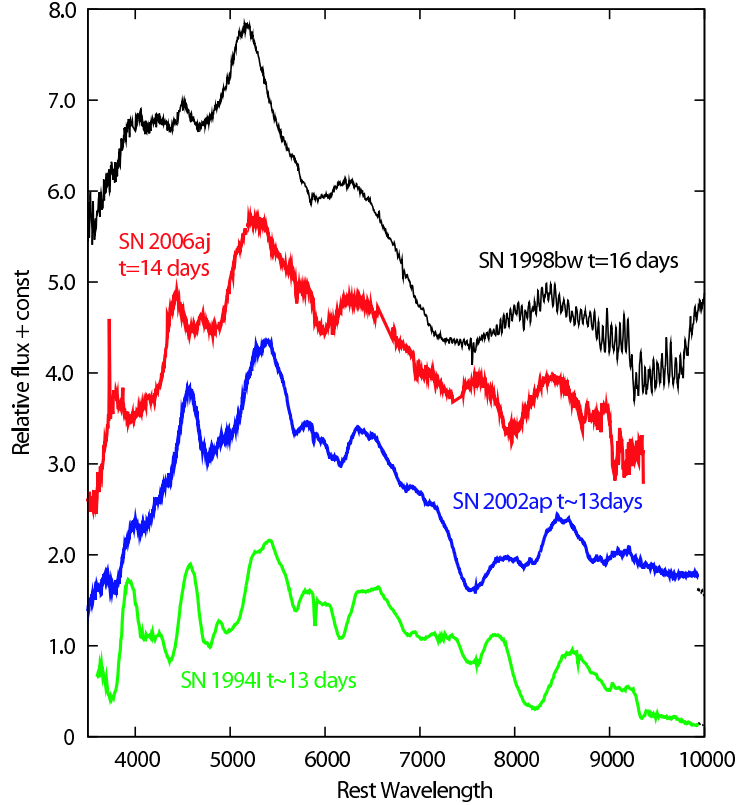


Fig. 1. – The spectra of 3 Hypernovae and 1 normal SN a few days before maximum. SN 1998bw/GRB 980425 represents the GRB-SNe. SN 2002ap is a non-GRB Hypernova. SN 2006aj is associated with XRF 060218, being similar to SN 2002ap. SN 1994I represents normal SNe.

(GRB 980425/SN 1998bw [16]; GRB 030329/SN 2003dh [54, 21]; GRB 031203/SN 2003lw [33]). Such GRB-SN connection is now revealing quite a large diversity as follows.

(1) GRB-SNe: The three SNe Ic associated with the above GRBs have similar properties; showing broader lines than normal SNe Ic (Fig. 1: so-called broad-lined SNe [66, 40]). These three GRB-SNe have been all found to be Hypernovae (HNe), i.e., very energetic supernovae, whose *isotropic* kinetic energy (KE) exceeds 10^{52} erg, about 10 times the KE of normal core-collapse SNe (hereafter $E_{51} = E/10^{51}$ erg) [24, 46, 48].

(2) Non-GRB HNe/SNe: These SNe show broad line features but are not associated with GRBs (SN 1997ef [25]; SN 2002ap [34]; SN 2003jd [35]). These are either less energetic than GRB-SNe, or observed off-axis.

(3) XRF-SNe: X-Ray Flash (XRF) 060218 has been found to be connected to SN Ic 2006aj [6, 51, 52]. The progenitor’s mass is estimated to be small enough to form a “neutron star-making SN” [37].

(4) Non-SN GRBs: In this review talk (Fig. 2; [50]), we pointed out that nucleosynthesis in HNe can explain some of the peculiar abundance patterns (such as the large Zn/Fe and Co/Fe ratios) in extremely metal-poor stars, which have long been mysteries.

Possible Types of SN-HN

- **Type Ib Hypernova ? (Helium in mixed WR)**
- **Type II Hypernova ?**
 - Rotating Black-Hole + H-rich Envelope (low metallicity?)

Faint SN Ibc ?

– Small ^{56}Ni (fallback) + No Shock Heating

Faint Hypernovae (fallback of ^{56}Ni) ?

Dark SN/HN (Long GRB + no SN)

Fig. 2. – The summary slide of this talk [50] posted on the Conference program page at <http://www.merate.mi.astro.it/docM/OAB/Research/SWIFT/sanservolo2006/>. A Dark SN/HN (long GRB with no SN) is predicted.

In particular, we have predicted that the “dark HN” (= “non-SN GRB” = long GRB with no SN) should exist and be responsible for the formation of the carbon-rich extremely (and hyper) metal-poor stars (see Fig. 2). After the Venice conference, the predicted “non-SN GRBs” have been actually discovered (GRB 060605 and 060614) [13, 17, 9, 18].

Here we summarize the properties and diversities of SNe connected to the above various types of GRBs as illustrated in Figure 3. The model parameters are summarized in Table I. We then point out the GRB/Hypernova - First Star connection through nucleosynthesis approach [49].

2. – GRBs

Figure 1 compares the spectra of GRB-HNe (SN 1998bw), non-GRB SN, XRF-SNe, and normal SN Ic. The spectrum of SN 1998bw has very broad lines. The strongest absorptions are Ti II-Fe II (shortwards of $\sim 4000\text{\AA}$), Fe II-Fe III (near 4500\AA), Si II (near 5700\AA), and O I-Ca II (between 7000 and 8000\AA). We calculate the synthetic spectra for ejecta models of bare C+O stars with various ejected mass M_{ej} and E . The large E/M_{ej} is required to reproduce the broad features.

The spectroscopic modelings are combined with the light curve (LC) modeling as seen in Figure 5 to give the estimates of M_{ej} and E . The timescale of the LC around maximum brightness reflects the timescale for optical photons to diffuse [2]. For larger M_{ej} and smaller E , the LC peaks later and the LC width becomes broader because it is more difficult for photons to escape.

From the synthetic spectra and light curves, it was interpreted as the explosion of a massive star, with $E_{51} \sim 30$ and $M_{\text{ej}} \sim 10M_{\odot}$ [24]. Also the very high luminosity of SN 1998bw indicates that a large amount of ^{56}Ni ($\sim 0.5M_{\odot}$) was synthesized in the explosion.

The ejected ^{56}Ni mass is estimated to be $M(^{56}\text{Ni}) \sim 0.3 - 0.7M_{\odot}$ (e.g., [36]) which is 4 to 10 times larger than typical SNe Ic ($M(^{56}\text{Ni}) \sim 0.07M_{\odot}$ [49]).

The other two GRB-SNe, 2003dh and 2003lw, are also characterized by the very broad

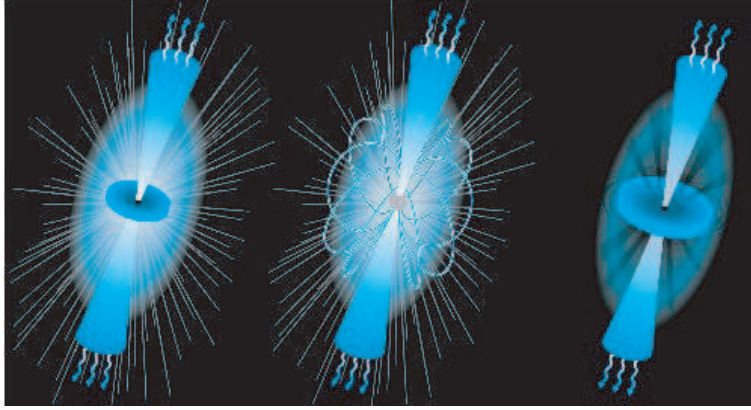


Fig. 3. – Illustrations of GRB-HNe, XRF-SNe, and no-SN-GRBs (from left to right).

line features and the very high luminosity. M_{ej} and E are estimated from synthetic spectra and light curves and summarized in Figure 11 [43, 10, 36]. It is clearly seen that GRB-SNe are the explosions of massive progenitor stars (with the main sequence mass of $M_{\text{ms}} \sim 35 - 50 M_{\odot}$), have large explosion kinetic energies ($E_{51} \sim 30 - 50$), synthesized large amounts of ^{56}Ni ($\sim 0.3 - 0.5 M_{\odot}$).

These GRB-associated HNe (GRB-HNe) are suggested to be the outcome of very energetic black hole (BH) forming explosions of massive stars (e.g., [24]).

Hypernovae are also characterized by asphericity from the observations of polarization and emission line features [64, 27, 29]. The explosion energy of the aspherical models for hypernovae tends to be smaller than the spherical models by a factor of 2 - 3, but still being as high as $E_{51} \gtrsim 10$ [31].

TABLE I. – *The models for Type Ic SNe and HNe (masses M are in unit of M_{\odot} and $E_{51} = E/10^{51}$ ergs).*

Name	M_{ms}	M_{ej}	E_{51}	$M(^{56}\text{Ni})$	E_{51}/M_{ej}	$M(v > 30,000 \text{ km s}^{-1})$
SN 1998bw	40	10.4	40	0.4	3.8	1.46
SN 2003dh	32.5	7	35	0.4	5	1.41
SN 2003lw	55	13	60	0.55	4.2	1.76
SN 1997ef	32.5	8.6	12.75	0.15	1.5	0.36
SN 2002ap	22.5	3.3	4	0.07	1.2	0.055
SN 2006aj	20	1.8	2	0.21	1.1	0.019
SN 1994I	14	1	1	0.07	1	0.0028

3. – Non-GRB Hypernovae/Supernovae

These HNe show spectral features similar to those of GRB-SNe but are not known to have been accompanied by a GRB. The estimated M_{ej} and E , obtained from synthetic light curves and spectra, show that there is a tendency for non-GRB HNe to have smaller M_{ej} , E , and lower luminosities as summarized in Table I and Figure 11.

SN 1997ef is found to be the HN class of energetic explosion, although E/M_{ej} is a factor 3 smaller than GRB-SNe (Fig. 12). It is not clear whether SN 1997ef is not associated with GRB because of this smaller E/M_{ej} or it was actually associated with the candidate GRB 971115.

SN 2002ap was not associated a GRB and no radio has been observed. It has similar spectral features, but narrower and redder (Fig. 1), which was modeled as a smaller energy explosion, with $E_{51} \sim 4$ and $M_{\text{ej}} \sim 3M_{\odot}$ [34].

The early time spectrum of SN 2003jd is similar to SN 2002ap. Interestingly, the its nebular spectra shows a double peak in O-emission lines [35]. This has exactly confirmed the theoretical prediction by the asymmetric explosion model [29]. In this case, the orientation effect might cause the non-detection of a GRB (see Mazzali et al. in this volume for more details.)

Whether the non-detection of GRBs is the effect of different orientations or of an intrinsic property is still a matter of debate, but there is a tendency for them to have smaller M_{ej} and E . SN 1997ef seems to be a marginal case.

4. – XRF–Supernovae

GRB060218 is the second closest event as ever (~ 140 Mpc). The GRB was weak [6] and classified as X-Ray Flash (XRF) because of its soft spectrum. The presence of SN 2006aj was soon confirmed[51, 39]. Here we summarize the properties of SN 2006aj by comparing with other SNe Ic.

SN 2006aj has several features that make it unique. It is less bright than the other GRB/SNe (Fig. 4). Its rapid photometric evolution is very similar to that of a dimmer, non-GRB SN 2002ap[34], but it is somewhat faster. Although its spectrum is characterized by broader absorption lines as in SN 1998bw and other GRB/SN, they are not as broad as those of SN 1998bw, and it is much more similar to that of SN 2002ap (Fig. 1). The most interesting property of SN 2006aj is surprisingly weak oxygen lines, much weaker than in Type Ic SNe.

4.1. Spectroscopic and Photometric Models. – By modeling the spectra and the light curve, we derive for SN 2006aj $M_{\text{ej}} \sim 2M_{\odot}$ and $E_{51} \sim 2$ as follows (Figs. 5 and 6). Lack of oxygen in the spectra indicates $\sim 1.3M_{\odot}$ of O, and oxygen is still the dominant element.

The strength of the OI λ 7774 line, which is the strongest oxygen line in optical wavelength, is sensitive to the temperature in the ejecta. Since the fraction of OI is larger in the lower temperature ejecta (although OII is still the dominant ionization state), the normal SNe Ib/c always show the strong OI absorption (see SN 1994I in Fig. 1) irrespective of the ejecta mass.

In more luminous SNe like GRB-SNe and SN 2006aj, the OI fraction tends to be smaller. However, if the ejecta are very massive, e.g., $\sim 10M_{\odot}$, the mass of OI is large enough to make the strong absorption (see SN 1998bw in Fig. 1). In the case of SN 2006aj, the temperature is larger than in normal SNe Ib/c. Therefore, the weak OI

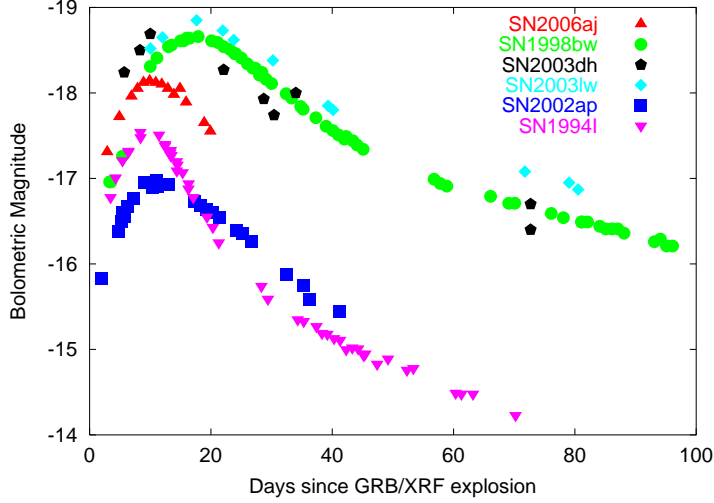


Fig. 4. – The bolometric light curves of GRB-SN (SNe 1998bw, 2003dh), non-GRB-SN (2002ap), XRF-SN (2006aj), and normal SNe Ic (1994I) are compared.

line indicates that the ejecta mass is not as massive as SN 1998bw, which supports our conclusion.

The spectroscopic results are confirmed through the light curve modeling (Fig. 5). We synthesize the theoretical light curve for the density and chemical abundance structure to compare with SN 2006aj. The best match is achieved with a total ^{56}Ni mass of $0.21M_{\odot}$ in which $0.02M_{\odot}$ is located above $20,000\text{km s}^{-1}$ (Fig. 4). The high-velocity ^{56}Ni is responsible for the fast rise of the light curve, because photons created can escape more easily. In a realistic asymmetric explosion, such high-velocity ^{56}Ni could abundantly be produced along the direction of the GRB jets [29, 30].

4.2. The Progenitor and Implications for XRF. – The properties of SN 2006aj (smaller E and smaller M_{ej}) suggest that SN 2006aj is not the same type of event as the other GRB-SNe known thus far. One possibility is that the initial mass of the progenitor star is much smaller than the other GRB-SNe, so that the collapse/explosion generated less energy. If M_{ms} is $\sim 20 - 25M_{\odot}$, the star would be at the boundary between collapse to a black hole or to a neutron star. In this mass range, there are indications of a spread in both E and the mass of ^{56}Ni synthesized [19]. The fact that a relatively large amount of ^{56}Ni is required in SN 2006aj possibly suggests that the star collapsed only to a neutron star because more core material would be available to synthesize ^{56}Ni in the case.

Although the kinetic energy of $E_{51} \sim 2$ is larger than the canonical value (1×10^{51} erg, [44]) in the mass range of $M_{\text{ms}} \sim 20 - 25M_{\odot}$, such an energy might be obtained from magnetar-type activity. It is conceivable that in this weaker explosion than typical GRB-SNe, the fraction of energy channeled to relativistic ejecta is smaller, giving rise to an XRF rather than a classical GRB.

Another case of a SN associated with an XRF has been reported (XRF030723) [12]. The putative SN, although its spectrum was not observed, was best consistent with the properties of SN 2002ap [57]. This may suggest that XRFs are associated with less

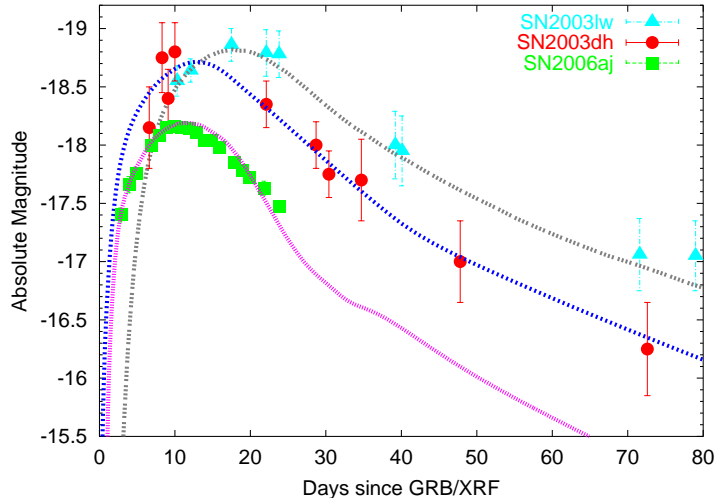


Fig. 5. – Theoretical bolometric light curves for SNe 2003dh, 2003lw, and 2006aj.

massive progenitor stars than those of canonical GRBs, and that the two groups may be differentiated by the formation of a neutron star [42] or a BH. Still, the progenitor star must have been thoroughly stripped of its H and He envelopes, which is a general property of all GRB-SNe and probably a requirement for the emission of a high energy transient. These facts may indicate that the progenitor is in a binary system.

If magnetars are related to the explosion mechanism, some short γ -ray repeaters energized by a magnetar [55, 56] may be remnants of GRB060218-like events. Magnetars could generate a GRB at two distinct times. As they are born, when they have a very large spin rate (~ 1 ms), an XRF (or a soft GRB) is produced as in SN 2006aj/GRB060218. Later (more than 1,000 yrs), when their spin rate is much slower, they could produce short-hard GRBs [22].

Stars of $M_{\text{ms}} \sim 20 - 25 M_{\odot}$ are much more common than stars of $M_{\text{ms}} \sim 35 - 50 M_{\odot}$, and so it is highly likely that events such as GRB060218 are much more common in nature than the highly energetic GRBs. They are, however, much more difficult to detect because they have a low γ -ray flux. The discovery of GRB060218/SN 2006aj suggests that there may be a wide range of properties of both the SN and the GRB in particular in this mass range. The continuing study of these intriguing events will be exciting and rewarding.

5. – Non-SN Gamma-Ray Bursts

For recently discovered nearby long-duration GRB 060505 ($z = 0.089$, [13]) and GRB 060614 ($z = 0.125$, [17, 13, 9, 18]), no SN has been detected. Upper limits to brightness of the possible SNe are about 100 times fainter than SN 1998bw. These correspond to upper limits to the ejected ^{56}Ni mass of $M(^{56}\text{Ni}) \sim 10^{-3} M_{\odot}$.

A small amount of ^{56}Ni ejection has been indicated in the faintness of several Type II SNe (SNe II, e.g., SN 1994W, [53]; and SN 1997D, [62]). The estimated E of these faint SNe II are very small ($E_{51} \lesssim 1$, [62]). These properties are well-reproduced by the

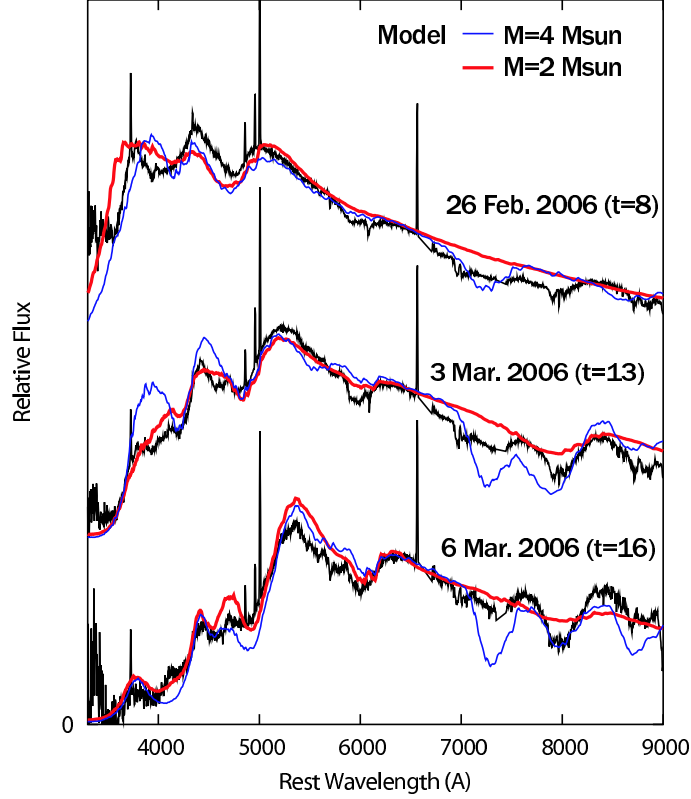


Fig. 6. – Synthetic spectra with a explosion model with $(M_{\text{ej}}, E_{51}) = (2.0M_{\odot}, 2.0)$ [gray solid lines] and $(4.0M_{\odot}, 9.0)$ [black dashed lines] compared with the observed spectra of SN 2006aj (solid lines).

spherical explosion models that undergo a large amount of fallback if E is sufficiently small [65, 26]. Thus these faint SN explosions with low E seem to be superficially irreconcilable to the formation of energetic GRBs [17]. We will show that the existence of a high-energy narrow jet which produces a GRB is compatible with a faint/dark and low E SN with little ^{56}Ni ejection.

Tominaga et al. [60] calculated the jet-induced explosions (e.g., [30, 41]) of the $40M_{\odot}$ stars [63, 59] by injecting the jets at a radius $R \sim 900$ km, corresponding to an enclosed mass of $M \sim 1.4M_{\odot}$. They investigated the dependence of nucleosynthesis outcome on \dot{E}_{dep} for a range of $\dot{E}_{\text{dep},51} \equiv \dot{E}_{\text{dep}}/10^{51}\text{ergs s}^{-1} = 0.3 - 1500$. The diversity of \dot{E}_{dep} is consistent with the wide range of the observed isotropic equivalent γ -ray energies and timescales of GRBs ([1] and references therein). Variations of activities of the central engines, possibly corresponding to different rotational velocities or magnetic fields, may well produce the variation of \dot{E}_{dep} .

After the jet injection is initiated, the shock fronts between the jets and the infalling material proceed outward in the stellar mantle. Figure 8 is a snapshot of the model with $\dot{E}_{\text{dep},51} = 15$ at 1 sec after the start of jet injection. When the jet injection ends, the jets have been decelerated by collisions with the dense stellar mantle and the shock has

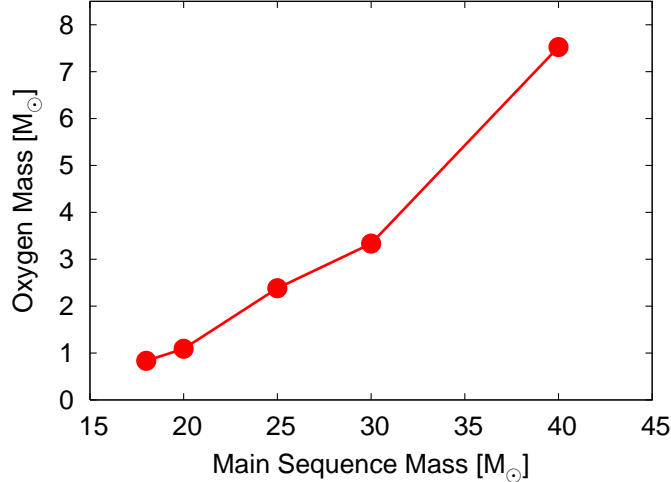


Fig. 7. – The synthesized oxygen mass as a function of the progenitor’s main-sequence mass.

become more spherical. The inner materials are ejected along the jet-axis but not along the equatorial plane.

5.1. ^{56}Ni Mass. – The top panel of Figure 9 shows the dependence of the ejected $M(^{56}\text{Ni})$ on the energy deposition rate \dot{E}_{dep} . For lower \dot{E}_{dep} , smaller $M(^{56}\text{Ni})$ is synthesized in explosive nucleosynthesis because of lower post-shock densities and temperatures (e.g., [30, 41, 32]).

If $\dot{E}_{\text{dep},51} \gtrsim 3$, the jet injection is initiated near the bottom of the C+O layer, leading to the synthesis of $M(^{56}\text{Ni}) \gtrsim 10^{-3}M_{\odot}$. If $\dot{E}_{\text{dep},51} < 3$, on the other hand, the jet injection is delayed and initiated near the surface of the C+O core; then the ejected ^{56}Ni is as small as $M(^{56}\text{Ni}) < 10^{-3}M_{\odot}$.

^{56}Ni contained in the relativistic jets is only $M(^{56}\text{Ni}) \sim 10^{-6} - 10^{-4}M_{\odot}$ because the total mass of the jets is $M_{\text{jet}} \sim 10^{-4}M_{\odot}$ in our model with $\Gamma_{\text{jet}} = 100$ and $E_{\text{dep}} = 1.5 \times 10^{52}$ ergs. Thus the ^{56}Ni production in the jets dominates over explosive nucleosynthesis in the stellar mantle only for $\dot{E}_{\text{dep},51} < 1.5$ in the present model.

5.2. GRB-HNe. – For high energy deposition rates ($\dot{E}_{\text{dep},51} \gtrsim 60$), the explosions synthesize large $M(^{56}\text{Ni})$ ($\gtrsim 0.1M_{\odot}$) being consistent with GRB-HNe. The remnant mass was $M_{\text{rem}}^{\text{start}} \sim 1.5M_{\odot}$ when the jet injection was started, but it grows as material is accreted from the equatorial plane. The final BH masses range from $M_{\text{BH}} = 10.8M_{\odot}$ for $\dot{E}_{\text{dep},51} = 60$ to $M_{\text{BH}} = 5.5M_{\odot}$ for $\dot{E}_{\text{dep},51} = 1500$, which are consistent with the observed masses of stellar-mass BHs [3]. The model with $\dot{E}_{\text{dep},51} = 300$ synthesizes $M(^{56}\text{Ni}) \sim 0.4M_{\odot}$ and the final mass of BH left after the explosion is $M_{\text{BH}} = 6.4M_{\odot}$.

5.3. Non-SN GRBs (060505 and 060614). – For low energy deposition rates ($\dot{E}_{\text{dep},51} < 3$), the ejected ^{56}Ni masses ($M(^{56}\text{Ni}) < 10^{-3}M_{\odot}$) are smaller than the upper limits for GRBs 060505 and 060614. The final BH mass is larger for smaller \dot{E}_{dep} . While the material ejected along the jet-direction involves those from the C+O core, the material along the equatorial plane fall back.

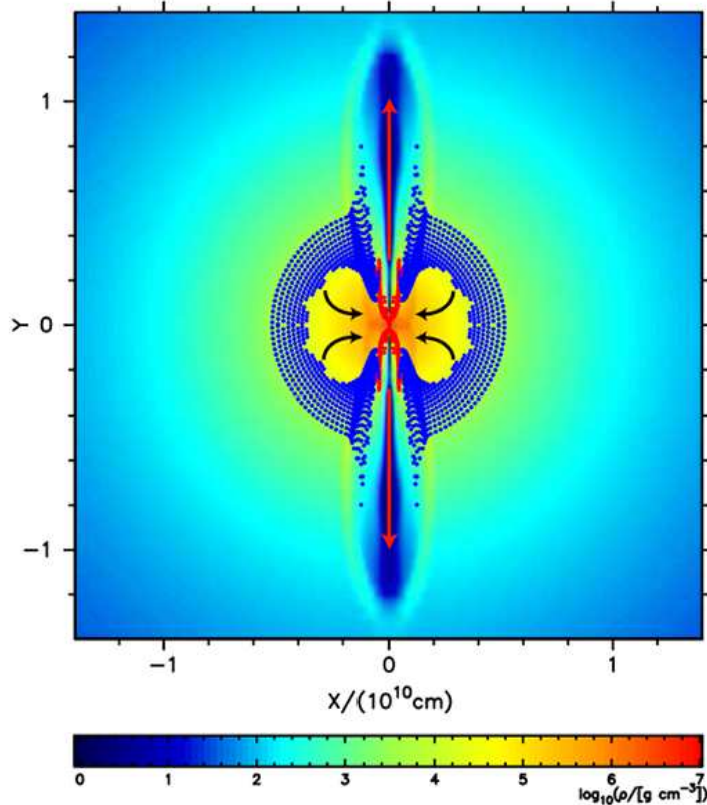


Fig. 8. – The density structure of the $40 M_{\odot}$ Pop III star explosion model of $\dot{E}_{\text{dep},51} = 15$ at 1 sec after the start of the jet injection. The jets penetrate the stellar mantle (*red arrows*) and material falls on the plane perpendicular to the jets (*black arrows*). The dots represent ejected Lagrangian elements dominated by Fe (^{56}Ni , *red*) and by O (*blue*).

If the explosion is viewed from the jet direction, we would observe GRB without SN re-brightening. This may be the situation for GRBs 060505 and 060614. In particular, for $\dot{E}_{\text{dep},51} < 1.5$, ^{56}Ni cannot be synthesized explosively and the jet component of the Fe-peak elements dominates the total yields (Fig. 9). The models eject very little $M(^{56}\text{Ni})$ ($\sim 10^{-6} M_{\odot}$).

5.4. GRBs with Faint or Sub-Luminous SNe. – For intermediate energy deposition rates ($3 \lesssim \dot{E}_{\text{dep},51} < 60$), the explosions eject $10^{-3} M_{\odot} \lesssim M(^{56}\text{Ni}) < 0.1 M_{\odot}$ and the final BH masses are $10.8 M_{\odot} \lesssim M_{\text{BH}} < 15.1 M_{\odot}$. The resulting SN is faint ($M(^{56}\text{Ni}) < 0.01 M_{\odot}$) or sub-luminous ($0.01 M_{\odot} \lesssim M(^{56}\text{Ni}) < 0.1 M_{\odot}$).

Nearby GRBs with faint or sub-luminous SNe have not been observed. This may be because they do not occur intrinsically in our neighborhood or because the number of observed cases is still too small. In the latter case, further observations may detect GRBs with a faint or sub-luminous SN.

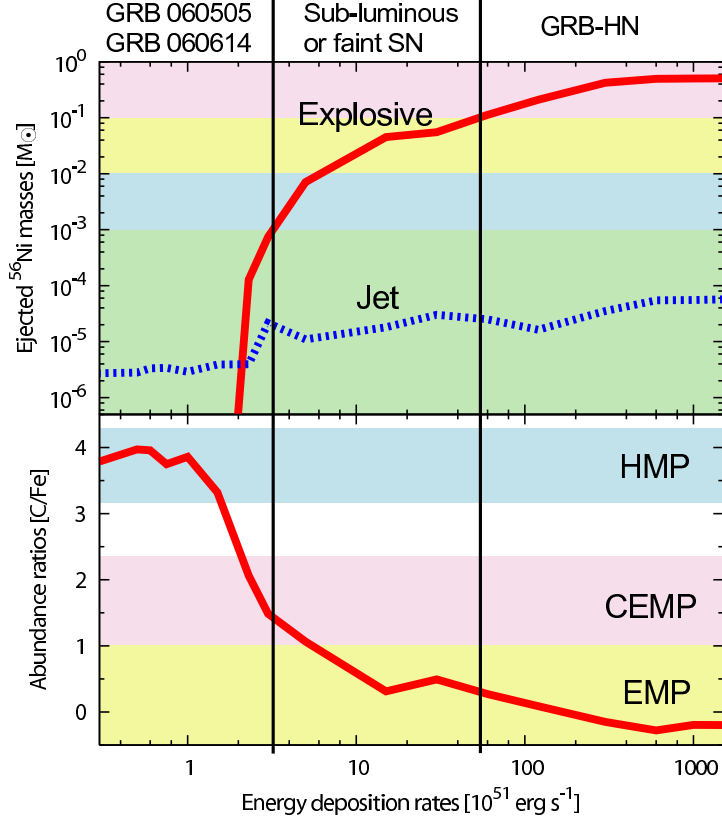


Fig. 9. – *Top*: the ejected ^{56}Ni mass (*red*: explosive nucleosynthesis products, *blue*: the jet contribution) as a function of the energy deposition rate. The background color shows the corresponding SNe (*red*: GRB-HNe, *yellow*: sub-luminous SNe, *blue*: faint SNe, *green*: GRBs 060505 and 060614). Vertical lines divide the resulting SNe according to their brightness. *Bottom*: the dependence of abundance ratio $[\text{C}/\text{Fe}]$ on the energy deposition rate. The background color shows the corresponding metal-poor stars (*yellow*: EMP, *red*: CEMP, *blue*: HMP stars).

5.5. Abundance Patterns of C-rich Metal-Poor Stars. – The bottom panel of Figure 9 shows the dependence of the abundance ratio $[\text{C}/\text{Fe}]$ on \dot{E}_{dep} . Lower \dot{E}_{dep} yields larger M_{BH} and thus larger $[\text{C}/\text{Fe}]$, because the infall decreases the amount of inner core material (Fe) relative to that of outer material (C) (see also [30]). As in the case of $M(^{56}\text{Ni})$, $[\text{C}/\text{Fe}]$ changes dramatically at $\dot{E}_{\text{dep},51} \sim 3$.

The abundance patterns of the EMP stars are good indicators of SN nucleosynthesis because the Galaxy was effectively unmixed at $[\text{Fe}/\text{H}] < -3$ (e.g., [61]). They are classified into three groups according to $[\text{C}/\text{Fe}]$:

- (1) $[\text{C}/\text{Fe}] \sim 0$, normal EMP stars ($-4 < [\text{Fe}/\text{H}] < -3$, e.g., [7]);
- (2) $[\text{C}/\text{Fe}] \gtrsim +1$, Carbon-enhanced EMP (CEMP) stars ($-4 < [\text{Fe}/\text{H}] < -3$, e.g., CS 22949–37 [11]);
- (3) $[\text{C}/\text{Fe}] \sim +4$, hyper metal-poor (HMP) stars ($[\text{Fe}/\text{H}] < -5$, e.g., HE 0107–5240 [8, 4]; HE 1327–2326 [15]).

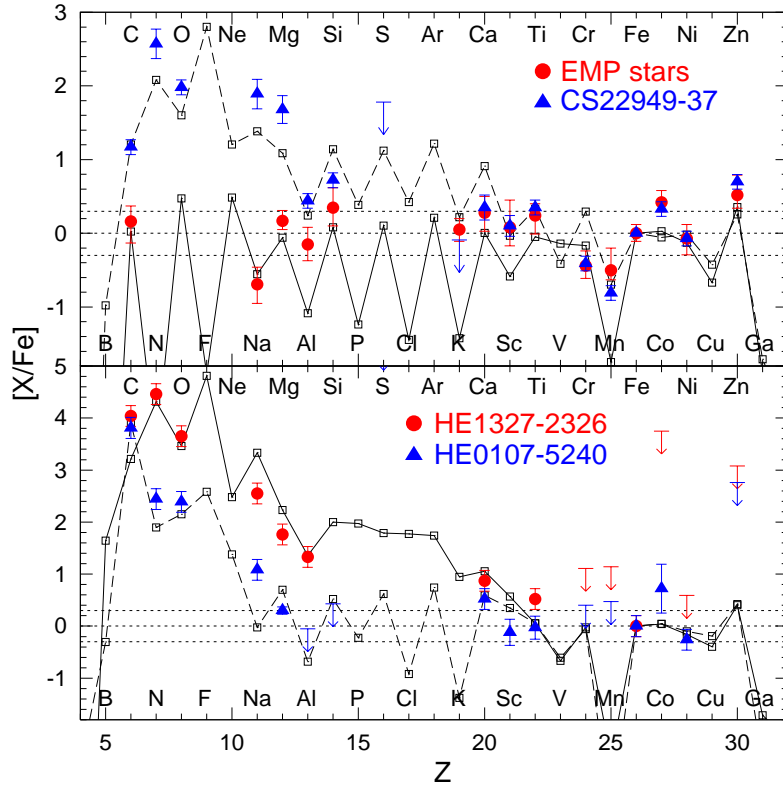


Fig. 10. – A comparison of the abundance patterns of metal-poor stars and of our models. *Top*: typical EMP (red dots, [7]) and CEMP (blue triangles, CS 22949–37, [11]) stars and models with $\dot{E}_{\text{dep},51} = 120$ (solid line) and $= 3.0$ (dashed line). *Bottom*: HMP stars: HE 1327–2326, (red dots, e.g., [15]), and HE 0107–5240, (blue triangles, [8, 4]) and models with $\dot{E}_{\text{dep},51} = 1.5$ (solid line) and $= 0.5$ (dashed line).

Figure 10 shows that the general abundance patterns of the normal EMP stars, the CEMP star CS 22949–37, and the HMP stars HE 0107–5240 and HE 1327–2326 are reproduced by models with $\dot{E}_{\text{dep},51} = 120, 3.0, 1.5,$ and 0.5 , respectively (see Table 1 for model parameters). The model for the normal EMP stars ejects $M(^{56}\text{Ni}) \sim 0.2M_{\odot}$, i.e. a factor of 2 less than SN 1998bw. On the other hand, the models for the CEMP and the HMP stars eject $M(^{56}\text{Ni}) \sim 8 \times 10^{-4}M_{\odot}$ and $4 \times 10^{-6}M_{\odot}$, respectively, which are always smaller than the upper limits for GRBs 060505 and 060614.

6. – Discussion

Figure 11 summarize the properties of core-collapse SNe as a function of the main-sequence mass M_{ms} of the progenitor star [47]. Figure 12 shows how the properties of these SNe depend on E/M_{ej} and the mass contained at the the expansion velocity exceeding $v = 30,000 \text{ km s}^{-1}$.

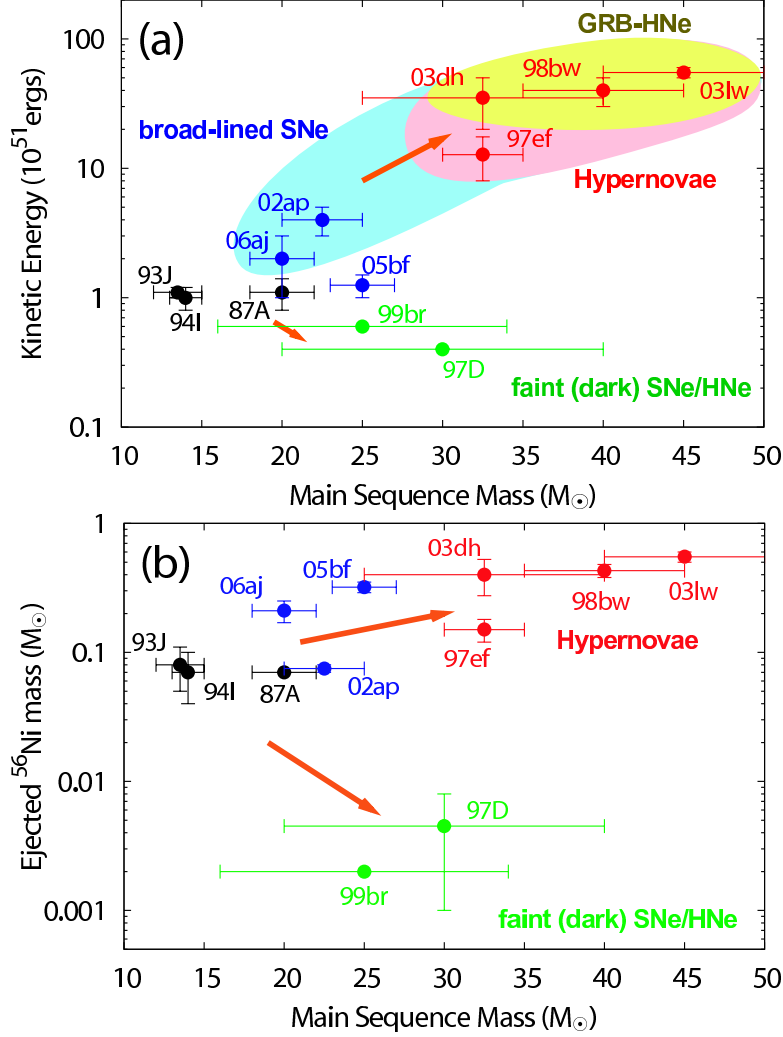


Fig. 11. – The kinetic explosion energy E and the ejected ^{56}Ni mass as a function of the main sequence mass M of the progenitors for several supernovae/hypernovae. SNe that are observed to show broad-line features are indicated. Hypernovae are the SNe with $E_{51} > 10$.

6.1. GRB, Hypernovae, Broad-Line features. – The broad-line SNe include both GRB-SNe and Non-GRB SNe.

(1) GRB vs. Non-GRB: Three GRB-SNe are all similar Hypernovae (i.e., $E_{51} \gtrsim 10$). Thus E could be closely related to the formation of GRBs. SN 1997ef seems to be a marginal case. As seen in Figure 12, E/M_{ej} could be more important because SN 1997ef has significantly smaller E/M_{ej} than GRB-SNe.

(2) Broad-Line features: The mass contained at $v > 30,000 \text{ km s}^{-1}$ (or even higher boundary velocity) might be critical in forming the broad-line features, although further modeling is required to clarify this point.

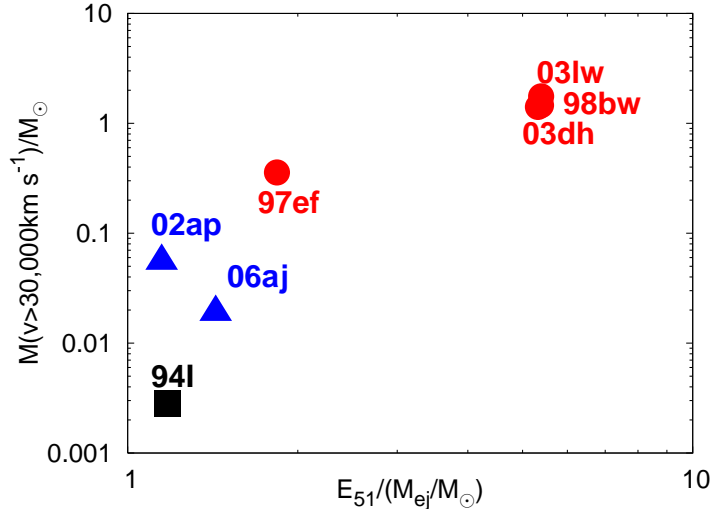


Fig. 12. – The mass (in unit of M_{\odot}) contained in the outer layer of the models where the expansion velocities exceed $v = 30,000 \text{ km s}^{-1}$ against $E_{51}/(M_{ej}/M_{\odot})$.

6.2. XRFs, GRBs, and SNe Ibc from the 20 - 25 M_{\odot} Progenitors. – The discovery of XRF 060218/SN 2006aj and their properties extend the GRB-HN connection to XRFs and to the HN progenitor mass as low as $\sim 20M_{\odot}$. The XRF 060218 may be driven by a neutron star rather than a black hole.

The final fate of 20 - 25 M_{\odot} stars show interesting variety. Even normal SN Ib 2005bf is very different from previously known SNe/HNe [58, 14]. This mass range corresponds to the transition from the NS formation to the BH formation. The NSs from this mass range could be much more active than those from lower mass range because of possibly much larger NS masses (near the maximum mass) or possibly large magnetic field (i.e., Magnetar). XRFs and GRBs from this mass range of 20 - 25 M_{\odot} might form a different population.

6.3. Hypernovae of Type II and Type Ib?. – Suppose that smaller losses of mass and angular momentum from low metallicity massive stars lead to the formation of more rapidly rotating NSs or BHs and thus more energetic explosions. Then we predict the existence of Type Ib and Type II HNe [20], as summarized in the slide of Figure 2 [50]

So far all observed HNe are of Type Ic. However, most of SNe Ic are suggested to have some He [5]. If even the small amount of radioactive ^{56}Ni is mixed in the He layer, the He feature should be seen [28, 45]. For HNe, the upper mass limit of He has been estimated to be $\sim 2M_{\odot}$ [34] for the case of no He mixing. If He features would be seen in future HN observations, it would provide an important constraint on the models, especially, the fully mixed WR models [68, 67, 38].

6.4. Hypernova-First Star Connection. – Based on the results in the earlier section, we suggest that the first generation supernovae were the explosion of ~ 20 -130 M_{\odot} stars and some of them produced C-rich, Fe-poor ejecta.

We have computed hydrodynamics and nucleosynthesis for the explosions induced by relativistic jets. We have shown that (1) the explosions with large E_{dep} are observed as

GRB-HNe and their yields can explain the abundances of normal EMP stars, and (2) the explosions with small \dot{E}_{dep} are observed as GRBs without bright SNe and can be responsible for the formation of the CEMP and the HMP stars. We thus propose that GRB-HNe and GRBs without bright SNe belong to a continuous series of BH-forming massive stellar deaths with the relativistic jets of different \dot{E}_{dep} .

A short GRB, probably the result of the merger of two compact objects (e.g., [23]), synthesizes virtually no ^{56}Ni because the ejecta must be too neutron-rich. In contrast, our model suggests that GRBs 060505 and 060614 produced $M(^{56}\text{Ni}) \sim 10^{-4} - 10^{-3} M_{\odot}$ or $\sim 10^{-6} M_{\odot}$. If such a GRB without a bright SN occurs in a very faint and nearby galaxy, our model predicts that some re-brightening due to the ^{56}Ni decay can be observed.

The nearby GRB-HNe and GRBs without bright SNe eject $M(^{56}\text{Ni}) \sim 0.3 - 0.7 M_{\odot}$ and $< 10^{-3} M_{\odot}$, respectively. The GRB-associated faint or sub-luminous SNe with $10^{-3} M_{\odot} \lesssim M(^{56}\text{Ni}) < 0.3 M_{\odot}$ have never been observed at close distances. Possible reasons may be that (1) they do not occur intrinsically, i.e., the energy deposition rate is bimodally distributed, or that (2) the number of observed nearby GRBs is still too small. For case (1), the GRB progenitors may be divided into two groups, e.g., with rapid or slow rotation and/or with strong or weak magnetic fields. For case (2), future observations will detect GRBs associated with a faint or sub-luminous SN.

* * *

This work has been supported in part by the Grant-in-Aid for Scientific Research (17030005, 17033002, 18104003, 18540231 for K.N.) and the 21st Century COE Program (QUEST) from the JSPS and MEXT of Japan.

REFERENCES

- [1] Amati, L., Della Valle, M., Frontera, F., Malesani, D., Guidorzi, C., Montanari, E., & Pian, E., *A&A* (2007) submitted (astro-ph/0607148)
- [2] Arnett, W. D. *ApJ* **253** (1982) 785
- [3] Baily, C.D., Jain, R.K., Coppi, P., & Orosz, J.A., *ApJ* **499** (1998) 367
- [4] Bessell, M. S., & Christlieb, N., in From Lithium to Uranium: Elemental Tracers of Early Cosmic Evolution. eds. Hill, V., François, P., & Primas, F. **228** (2005) 237
- [5] Branch, D., Jeffery, D.J., Timothy, R.Y., & Baron, E., *PASP* **118** (2006) 791
- [6] Campana, S., et al., *Nature* **442** (2006) 1008
- [7] Cayrel, R., et al., *A&A* **416** (2004) 1117
- [8] Christlieb, N., et al., *Nature* **419** (2002) 904
- [9] Della Valle, M., et al., 2006, *Nature* **444** (2006) 1050
- [10] Deng, J., et al. *Astrophys. J.* **624**, (2005) 898.
- [11] Depagne, E., et al., *A&A* , **390** (2002) 187
- [12] Fynbo, J.P.U. et al., *Astrophys. J.* **609** (2004) 962–971
- [13] Fynbo, J.P.U., et al., *Nature* **444** (2006) 1047
- [14] Folatelli, G., et al., *ApJ* **641** (2006) 1039
- [15] Frebel, A., et al., *Nature* **434** (2005) 871
- [16] Galama, T., et al., *Nature* **395** (1998) 670
- [17] Gal-Yam, A., et al., *Nature* **444** (2006) 1053
- [18] Gehrels, N., et al., *Nature* **444** (2006) 1044
- [19] Hamuy, M., *ApJ* **582** (2003) 905
- [20] Hamuy, M., Contreras, C., Gonzalez, S., Krzeminski, W. 2005, IAUCirc., 8520
- [21] Hjorth, J., et al., *Nature* **423** (2003) 847
- [22] Hurley, K., et al. *Nature* **434** (2005) 1098–1103

- [23] Gehrels, N., *et al.*, *Nature* **437** (2005) 851
- [24] Iwamoto, K., Mazzali, P.A., Nomoto, K., *et al.*, *Nature* **395** (1998) 672
- [25] Iwamoto, K., Nakamura, T., Nomoto, K., *et al.*, *ApJ* **534** (2000) 660
- [26] Iwamoto, N., Umeda, H., Tominaga, N., Nomoto, K., & Maeda, K., *Science* **309** (2005) 451
- [27] Kawabata, K., *et al.* *ApJ* **580** (2002) L39
- [28] Lucy, L.B., *ApJ* **383** (1991) 308
- [29] Maeda, K., Nakamura, T., Nomoto, K., Mazzali, P.A., Patat, F., & Hachisu, I. *ApJ* **565** (2002) 405
- [30] Maeda, K. & Nomoto, K., *ApJ* **598** (2003) 1163
- [31] Maeda, K., Mazzali, P.A., & Nomoto, K., *ApJ* **645** (2006) 1331
- [32] Maeda, K., & Tominaga, N., *ApJ* (2007) submitted
- [33] Malesani, J., *et al.*, *ApJ* **609** (2006) L5
- [34] Mazzali, P.A., Deng, J., Maeda, K., Nomoto, K., *et al.*, *ApJ* **572** (2002) L61
- [35] Mazzali, P. A., Kawabata, K.S., Maeda, K., *et al.* *Science* **308** (2005) 1284
- [36] Mazzali, P. A., *et al.*, *ApJ* **645** (2006a) 1323
- [37] Mazzali, P.A., Deng, J., Nomoto, K., *et al.*, *Nature* **442** (2006b) 1018
- [38] Meynet, G., & Maeder, A., *A&A* (2007) in press (astro-ph/0701494)
- [39] Modjaz, M., *et al.* *ApJ* **645** (2006) L21
- [40] Modjaz, M., *et al.*, *AJ* (2007) submitted (astro-ph/0701246)
- [41] Nagataki, S., Mizuta, A., & Sato, K., *ApJ* **647** (2006) 1255
- [42] Nakamura, T., *Prog. Theor. Phys.* **100** (1998) 921
- [43] Nakamura, T., Mazzali, P.A., Nomoto, K., Iwamoto, K., *ApJ* **550** (2001) 991
- [44] Nomoto, K., *et al.* *Nature* **371** (1994) 227
- [45] Nomoto, K., Iwamoto, K., & Suzuki, T. *Phys. Rep.* **256** (1995) 173
- [46] Nomoto, K., Mazzali, P.A., Nakamura, T., *et al.*, in *Supernovae and Gamma Ray Bursts*, eds. M. Livio *et al.* (Cambridge Univ. Press) (2001) 144 (astro-ph/0003077)
- [47] Nomoto, K., *et al.*, in *IAU Symp 212, A massive Star Odyssey, from Main Sequence to Supernova*, eds. V.D. Hucht, *et al.* (San Francisco: ASP) (2003) 395 (astro-ph/0209064)
- [48] Nomoto, K., *et al.*, in *Stellar Collapse*, ed. C.L. Fryer (Astrophysics and Space Science: Kluwer) (2004) 277 (astro-ph/0308136)
- [49] Nomoto, K., Tominaga, N., Umeda, H., Kobayashi, C., & Maeda, K., *Nuclear Phys A*, **777**, 424 (astro-ph/0605725)
- [50] Nomoto, K., A review talk at the Conference “Swift and GRBs: Unveiling the Relativistic Universe” (Venice, 2006 June 5-9); the ppt file available from “program” at <http://www.merate.mi.astro.it/docM/OAB/Research/SWIFT/sanservolo2006/>
- [51] Pian, E., *et al.*, *Nature* **442** (2006) 1011
- [52] Soderberg, A.M., *et al.* *Nature* **442** (2006) 1014
- [53] Sollerman, J., Cumming, R., & Lundqvist, P., *ApJ* **493** (1998) 933
- [54] Stanek, K.Z., *et al.*, *ApJ* **591** (2003) L17
- [55] Thompson, T.A., & Duncan, R.C. *Mon. Not. Royal Astron. Soc.* **275** (1995) 255- 300
- [56] Thompson, T.A., Chang, P., & Quataert, E. *ApJ* **611** (2004) 380
- [57] Tominaga, N. *et al.* *ApJ* **612** (2004) L105
- [58] Tominaga, N. *et al.* *ApJ* **633** (2005) L97
- [59] Tominaga, N., Umeda, H., Nomoto, K. *ApJ* **660** (2007a) in press (astro-ph/0701381)
- [60] Tominaga, N., Maeda, K., Umeda, H., Nomoto, K., Tanaka, M., Iwamoto, N., Suzuki, T., & Mazzali, P. A. *ApJ* **657** (2007b) in press (astro-ph/0702471)
- [61] Tumlinson, J., *ApJ* **641** (2006) 1
- [62] Turatto, M., Mazzali, P.A., Young, T., Nomoto, K., *et al.*, *ApJ* **498** (1998) L129
- [63] Umeda, H., & Nomoto, K., *ApJ* **619** (2005) 427
- [64] Wang, L., Baade, D., Höflich, P., & Wheeler, J.C., *ApJ* **592** (2003) 457
- [65] Woosley, S. E., & Weaver, T. A., *ApJS* **101** (1995) 181
- [66] Woosley, S. E., & Bloom, J.S., *ARA&A* **44** (2006) 507
- [67] Woosley, S. E., & Heger, A., *ApJ* **637** (2006) 914
- [68] Yoon, S.-C., & Langer, N., *A&A* **443** (2006) 643